EVALUATE THE RISK OF HYDRATE BLOCKAGE INBEND FLOWLINES

H. Kh. Ben Mahmud
Department of Petroleum Engineering, Curtin University, Sarawak, Malaysia
E-Mail: hisham@curtin.edu.my

ABSTRACT

As oil and gas developments are moving into deeper waters, production strategies are becoming more challenging due to the aggressive environment. Generally, offshore wells have flow lines that transport hydrocarbon between the platforms, manifolds, and onshore facilities are normally lying on the sea bed. In such configuration where the flow lines are curved, there is a high risk of water accumulation at the low spot sections during shutdown operations. A multiphase Computational Fluid Dynamic (CFD) model based on a Volume of Fluid (VOF) approach is employed to investigate the effect of restart gas superficial velocity at a different liquid patching on the flow pattern within a long pipeline. The flow pattern obtained from the CFD simulations compared well with Baker flow map. Therefore, CFD is demonstrated to be an efficient tool to predict adequately the flow behavior in such pipe flow system. The CFD generated flow pattern map allows for the risk assessment of hydrate blockage, thus pointing out the conditions where the risk is either low or high.

Keywords: multiphase flow, CFD, flow regime, bend pipeline.

INTRODUCTION

Exploration and production of oil and gas have moved into deep offshore waters with extreme conditions such as high pressure and low temperature since onshore reservoirs have been depleted. Typically the flowlines are used to transport the crude oil and gas from offshore to the processing facilities. In such systems, two–phase flow is more likely to take place during the transportation of hydrocarbons and gas condensate. Different flow patterns are expected to be generated, such as stratified, dispersed, slug flow etc.

It has been recognized that a new flow assurance approach is required to reduce the cost of hydrate mitigation strategies for the development of offshore deep water gas fields [1]. The concept of a risk based management of hydrates in pipelines is gaining acceptance in the oil and gas production community, based on the observation that the presence of hydrates does not always lead to pipeline blockages. Such approach must be necessarily built upon a sound knowledge of the mechanisms that govern hydrate formation kinetics and pipe clogging in gas production flow lines. Most of the research on hydrates behavior in flow lines has been limited to oil dominated systems in which the prevailing phase is black-oil or condensate. On the contrary, in gas flow lines, liquids (water and hydrocarbons) are usually present in small amounts which may increase with the production time [11].

Several studies have been conducted on two-phase flow in the conduit with different orientation angles (horizontal, vertical, and inclined) [2, 5, 6 and 9]. Therefore, the pipeline configuration is typically curved based on the sea floor topography. The accumulated water is most likely to accumulate in the low sections, which can lead to a high risk of hydrate formation during restart operations. The consequence of this can result in a blockage to the pipeline, which is considered a very important challenge to the offshore deep-water development. The earlier practice of hydrate control strategy is usually based only on hydrate equilibrium data provided, without considering the other system features, such as the physical design of the production system, fluid properties, and two-phase distribution. The consequence of this could lead to quite a conservative approach providing a significant negative impact on the project economy.

The current state-of-the art in the subject of hydrate control has not yet developed to establish criteria and an experimental methodology that would assist us to find conclusively whether safe operation within the hydrate zone (expressed by pressure-temperature plot) is possible or not. Few cases are reported where certain production systems have been sufficiently operated inside the hydrate area. Moreover, the cause of such behaviour is due to the natural surfactants, which exist with the crude oil [7].

Some authors [4, 7, and 8] have conducted a theoretical and experimental study for two-phase flow in a curved pipeline to investigate the hydrate plugging. The author studied various parameters, such as levels of stagnant liquid before restart, different gas restart velocities, pipe geometry, and different fluid systems (gas–water, and gas–water-oil), to examine the impact on hydrate plugging. It was found that the most significant case is at the low restart gas velocity throughout the accumulated stagnant water, where the plugging took place immediately and was controlled by the gas flow rate.

In the case of three phases, it was found that the oil layer can delay the plugging time or even prevent it, especially in the case of low water level, while at a high gas velocity no hydrate plugging was noted. Two different flow patterns were observed, these were dispersed and segregated flow. Furthermore, low gas restart velocities had a significant impact on the plugging tendency and also the water level plays a crucial role in the hydrate plugging in which the probability of hydrate formation is proportional to the water level. Furthermore, the plug can take place at a low water fraction, depending on the operating conditions and the pipe geometry. The result obtained provides some preliminary input to the actual

www.arpnjournals.com

field operations. Therefore, more research is needed in order to investigate the risk of hydrate plugging in different pipe geometries. Such systems of multiphase flow require a better understanding of multiphase transient flow patterns to assist in understanding the mechanisms of hydrate plug formation.

Furthermore, natural gas hydrate behaviour was investigated [11] in a gas pipeline (1 inch ID and 40 m long) with less than 10% liquid load. The hydrodynamic condition of the flow pattern was set to achieve wavy and annular flow regimes (moderate to high velocity) typical of gas production pipelines. The obtained results showed a complex, fast evolution of the hydrates over time occurring at a quite short period of time. Such result provided some information from the pressure drop profiles together with visual observations and a preliminary description of the phenomena taking place at steady-state and transient conditions initiative implantation to mathematical model. It has been demonstrated that useful information can be extracted from the pressure drop profiles together with visual observations and a preliminary description of the phenomena taking place at steady-state and transient conditions has been provided as a first step to the implementation of a mathematical model.

MULTIPHASE FLOW MODELLING

In order to study the hydrodynamics of droplets and flow patterns in horizontal pipelines, including low spots, an existing Computational Fluid Dynamic (CFD) code is used. For this purpose, the Volume of Fluid (VOF) model in the Eulerian framework for both phases with interface forces reformulation based on a volumetric basis is chosen for the two–phase flow simulation, in which the grid is fixed and the fluids are assumed to behave as continuous media [10], as will be illustrated next.

Solution procedure

The VOF model in ANSYS FLUENT 12.1 has been used to simulate the flow pattern and the droplet formation. In this model, the progress of gas–liquid interface is tracked using the distribution of the liquid fraction (α_l) in the computational cell. It is equal to zero in the gas phase and unity in the liquid phase. However, the interface of two–phase presents in the cell, where the liquid fraction ranges from 0−1. The finite volume discretisation scheme is employed for interface tracking. There are different discretisation schemes available with the explicit scheme for VOF where the CICSAM method was used to track the interface accurately. The surface tension was taken into account and given a constant value (0.073 N/m), and the k–ε turbulence model was applied to model the phase turbulence.

Equation of continuity (conservation of mass)

$$\frac{\partial}{\partial t}(\rho) + \nabla \cdot (\rho u_i) = 0 \tag{1}$$

Conservation of momentum (Navier-Stokes Equation)

One momentum equation is shared by all phases, and is solved all through the entire domain.

$$\frac{\partial}{\partial t}(\rho u_i) + \nabla \cdot (\rho u_i u_j) = -\nabla p + \nabla \cdot [\mu(\nabla u_i + \nabla u_j)] + \rho g_i + F_i \tag{2}$$

The term on the left hand side represents the convection and the other four terms on the right side represent the pressure, diffusion, the gravity and the external body force, respectively.

The volume fraction equation

The interface tracking between two phases of gas–liquid is achieved via solving the continuity equations of the liquid phase volume fraction, which can be written as:

$$\frac{\partial \alpha_l}{\partial t} + (U_i \cdot \nabla)\alpha_l = 0 \tag{3}$$

where the gas phase volume fraction is calculated based on the following constraint:

$$\alpha_g + \alpha_l = 1 \tag{4}$$

where α_g and α_l are the volume fraction of gas and liquid phase, respectively.

Turbulence model

The turbulence model of k-ε was utilized to model the turbulence in the continuous phase (gas). A turbulence model is commonly used for simulating turbulence eddies. This model takes into account the transport of turbulence velocity and length scale. It utilizes a transport equation for the length scale, which provides a distribution of the length scale even in the case of complex flow, such as two-phase flow in a pipeline, which the present research is concerned.

Physical properties

At any given cell, the properties and variables of gas and liquid are obtained either by the volume fraction contributions or presented purely. However, the two-phase mixture properties are found by the existence of the gas–liquid phase in each control volume. The mixture density and viscosity in each cell can be expressed by:

$$\rho_{mix} = \alpha_l \rho_l + \alpha_g \rho_g = \alpha_l \rho_l + (1 - \alpha_l)\rho_g \tag{5}$$

$$\mu_{mix} = \alpha_l \mu_l + \alpha_g \mu_g = \alpha_l \mu_l + (1 - \alpha_l)\mu_g \tag{6}$$

where ρ_l, μ_l and ρ_g, μ_g are the density and viscosity of liquid and gas phase.

www.arpnjournals.com

Differencing scheme/solution strategy and convergence criterion

The momentum equation was solved using a first order up-wind differencing scheme, while the scheme of Pressure Implicit with Splitting of Operators (PISO) pressure-velocity coupling was utilized for the pressure-velocity coupling scheme, as is recommended for usual transient calculation. The PRESTO scheme was used for pressure discretisation. As large body forces such as surface tension and gravity take place in the multiphase flows, the pressure gradient and body force expressions into the equation of momentum were almost in equilibrium compared to the small contributions of viscous and convective terms. Segregated algorithms converge poorly unless partial equilibrium of body forces and pressure gradient are taken into consideration.

The equation of liquid volume fraction was solved by applying an explicit time-marching scheme, and the maximum Counter number was set to 0.25. The values of under relaxation factors for momentum and pressure were 0.7 and 0.3, respectively. With respect to turbulence parameters, intensity and hydraulic diameter specifications were employed. A time step value of 0.001s was used during the simulations and is found to be sufficient to produce results independent of the choice of time step and thus utilized here.

DESCIPTION OF FLOWLINE CONDITIONS

To investigate the flow pattern and hydrodynamic behaviour of continuous droplets forming in a pipeline, different sets of simulations were performed in a 2-D approach using VOF model. The simulations were carried out in a pipeline with D = 0.5 m, and L= 55 m. The pipe is divided into two sections, where the low point section is approximately 10 m long with 1 m depth and the horizontal section is 45 m, which was filled with pure gas. These sections are shown in (Figure-1a) in which the low section was patched by an initial liquid level of 0.2 m (see Figure-1b).

The simulations were performed with a fixed mesh size, which was coarse at the low section and finer at the horizontal section in order to capture the flow pattern and the drop formation. Table-1 summarizes the physical properties of water and air that were used in this study. For all simulations, a no-slip condition was applied to the pipe walls and the influence of gravitational force was taken into account. At the pipe inlet, a velocity inlet boundary condition was employed to define the actual velocity of each phase as written in equation (7), and a pressure outlet boundary was imposed at the pipe outlet. All simulations were performed under the atmospheric pressure and room temperature, where [1] flow map was used for the flow pattern validation.

$$U_g = \frac{U_{s,g}}{1 - \alpha_{w}} U_w = \frac{U_{s,w}}{\alpha_{w}}$$

(7)#

RESULTS

Examination of turbulence models

Several turbulence models are available for utilization. Each turbulence model has advantages, disadvantages, limitations, and appropriate flow regimes. A large family of turbulence models exists in the literature, yet there are no quantitative guidelines for choosing an appropriate turbulence model for a multiphase flow. This section focuses on an assessment of three turbulence models, which are standard k-ε, RNG k-ε, and realizable k-ε. The model tests were conducted in a horizontal pipe having an internal diameter of 0.5 m and a length of 7 m to examine the result of each turbulence model, in which the best model result will be chosen for a grid independent test.

Figures 2 and 3 illustrate the relationship between the pressure gradient and liquid holdup against superficial water velocity at constant superficial air velocity of 20 m/s. It can be noted that RNG k-ε model had close agreement with the experimental data [13] in terms of pressure gradient and liquid holdup, and had less percentage of error. Therefore, this model has been chosen for further sensitivity analysis.

Grid-independent test

The aim of the grid–independent test is to verify the minimum grid resolution required to generate a solution that is independent of the grid used. In this test, the initial value of liquid volume fraction was calculated using [12] correlation. Three different mesh sizes were used for grid generation, which were 110,330, 204,300, and 401,200, respectively. Table-2 shows a comparison between different three mesh sizes using RNG k-ε turbulence model with respect to the experimental data in which the pressure gradient was chosen at a constant superficial gas and liquid velocity. The CFD pressure gradient decreases as the grids become finer. The result indicates that the mesh cell number of 204,300 is acceptable compared with mesh size of 401,200. In general, a total of 204, 300 cells are acceptable for the pipe meshing.

Effect of superficial gas velocity

In order to investigate the effect of gas superficial velocity on the flow pattern, simulations of air-water flow were performed with different restart gas velocities, ranging from 5-20 m/s, and with constant patched liquid of 0.2 m. Low restart gas superficial velocity of 5 m/s, created a slow gas-liquid interface displacement until it reached to the pipe horizontal section. It took approximately 1 sec as shown in (Figure-4a), while some of liquid returned to the low section due to not enough acceleration. Therefore, some of the water was observed in the low section (see Figure-5a). The remainder settled down into the horizontal section as a very thin film of a few millimetres thickness, and reached to the end of the pipe. At medium gas superficial velocity of 10 m/s, the liquid in the low point reached the horizontal section

www.arpnjournals.com

within around 0.5 sec as shown in (Figure-4b), where the water phase was not seen in the low section.
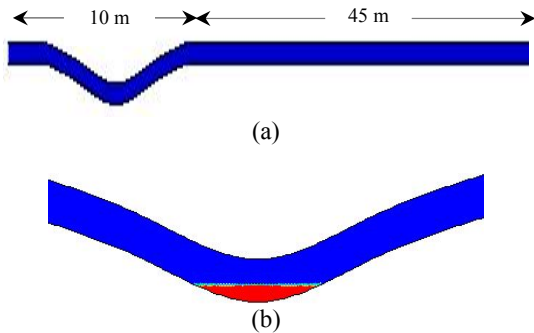
Figure-1. (a) Pipeline schematic and (b) Initial patched liquid phase at 20cm.

Table-1. Physical properties of water and air at ambient condition.

Fluid	ρ (kg/m^3)	μ (Pa.s)	σ (N/m)
Water	1000	0.001	0.073
Air	1.225	1.789×10^{-5}	

All of the liquid was carried over and was located in the horizontal section, in which the interface configuration was flat, as seen in (Figure-5b). This is a similar interface configuration that was observed in the case of 5 m/s. Therefore, for low liquid loading simulations with 5 and 10m/s, the gas-liquid interface remained almost flat. This represented a situation of a stratified flow. At higher gas superficial velocities of 15 and 20 m/s, most of the water in the low spot was taken out quickly, within less than 0.5 sec, as shown in (Figure-6a). As a result, the water was accumulated, remained in the horizontal section, and formed a thin film on the bottom pipe wall before it was dispersed.

The high gas velocity, therefore, generates more turbulence and penetrates the liquid phase with a much stronger force, when compared to low and medium velocities. However, at a high gas velocity of 15 m/s,
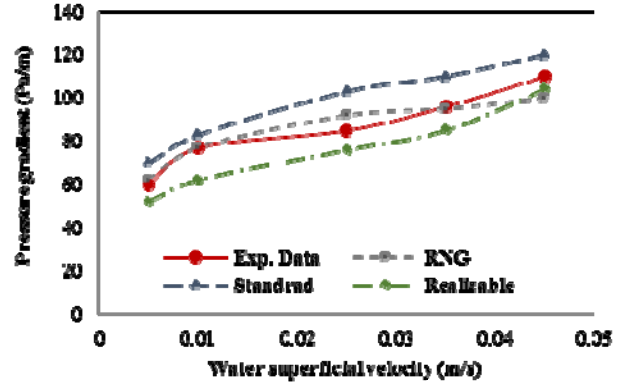
Figure-2. Shows the comparison of pressure gradient between the experimental data and different turbulence k-ε models.
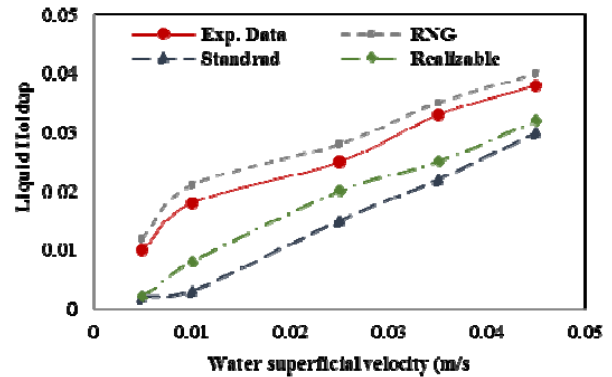
Figure-3. Shows the comparison of liquid holdup between the experimental data and different turbulence k-ε models.

Table-2. Effect of grid size on pressure drop using RNG k-ε model at constant superficial water velocity 0.025m/s.

Mesh	Gas superficial velocity (m/s)					
	15		20		25	
	Pressure gradient (Pa/m)					
	Exp.	CFD	Exp.	CFD	Exp.	CFD
110, 330	46.9	61.4	89.1	102.2	177.2	195.5
204, 300	46.9	53.6	89.1	92.5	177.2	180.3
401, 200	46.9	51.9	89.1	90.6	177.2	165.7

a dispersed or an annular flow, it was observed as droplets flow in the gas phase. Additionally, a small amount of liquid film covered the circumference of the pipe, as shown in (Figure-6b).

The superficial gas velocity of 20 m/s formed tiny drops at the tube outlet, and more drops were expected to form as the film continues to flow. The generated flow was considered as churn flow, as shown in (Figure-6c). The low liquid patching, however, illustrates the risk for hydrate plugging at low superficial gas velocities of 5 and 10 m/s simulations, due to the flow pattern observation. While the risk of hydrate plugging is

www.arpnjournals.com

not likely to happen due to the turbulence, which is generated by high gas velocity, it leads to delay the aggregation process of particles and the pipe blockage.

(a)

(b)
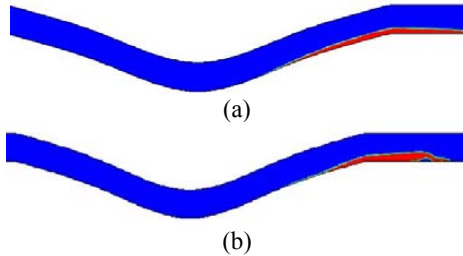
Figure-4. Displacement of water from the low point for (a) 5m/s and (b) 10m/s.

(a) Water is remaining in the low section after 35 sec, and creates flat interface.

(b) Interface between gas-liquid is flat at the end of pipe after 15 sec for 10m/s.
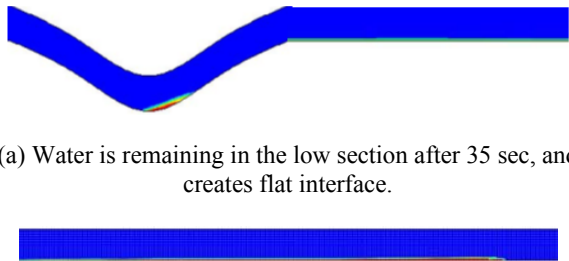
Figure-5. Sketch of water distribution with 5 and 10m/s gas velocity.
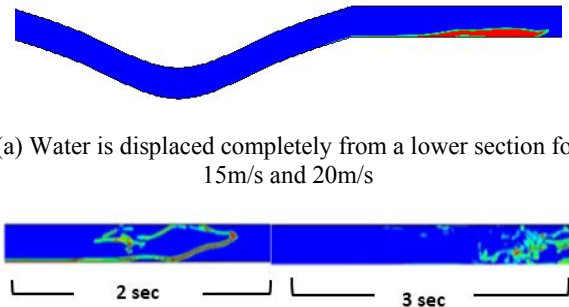
(a) Water is displaced completely from a lower section for 15m/s and 20m/s

(b) Liquid film configuration after 2 sec and 3 sec, it is clear the flow becomes dispersed/or annular.
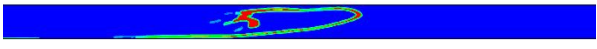
(c) The liquid film is lifted up and started to form droplets at the end of pipe for 20m/s.

Figure-6. Water distributions with high restart gas velocity.

COMPARE FLOW PATTERN SIMULATION WITH A FLOW MAP

In this work Baker's flow map in (Figure-7) is used to identify and compare the obtained flow pattern as a result of CFD two-phase flow simulation. The flow chart demonstrates the various boundaries of flow pattern zones as functions of a mass flux of gas and the ratio of liquid and gas phase which are expressed by (G) and (L/G) respectively. The dimensionless parameters ψ and λ are expressed by Equation (8) and (9), respectively.

$$\psi = \frac{g_w}{g}\left[\left(\frac{\mu_L}{\mu_w}\right)\left(\frac{\varrho_w}{\varrho_L}\right)^2\right]^{\frac{1}{3}}$$

(8)

$$\lambda = \left[\left(\frac{\varrho_g}{\varrho_a}\right)\left(\frac{\varrho_L}{\varrho_w}\right)^2\right]^{\frac{1}{2}}$$

(9)

In all simulation cases, the flow pattern of air-water flow was obtained under the atmospheric pressure and room temperature. The mass flux of each phase of air and water was calculated to find out the corresponding flow pattern according to the Baker flow map. Based on the physical properties of each phase of air and water, the dimensionless parameters (ψ, λ) are equal to 1 in this situation. In the case of low liquid patching, Table-3 presents the flow pattern obtained from different cases of simulation.

As can be seen from Table-3 and (figure-7) the predicted flow patterns using the Baker chart are quite adequate compared with the CFD simulations, especially at low and medium gas velocities of 5 and 10 m/s. At higher gas velocities all the obtained flow patterns are not predicted accurately with the flow pattern, which is expected from the Baker flow map. This could be due to the air-water flow simulation was performed in 2D geometry instead of 3D, which predicts the flow pattern more accurately. Alternatively it could also be due to the flow map which is typically constructed based on specific operating conditions.

Table-3. Predicted flow patterns for low liquid patching.

G (kg/s.m^2)	L (kg/s.m^2)	L/G	Us, g (m/s)	Re	Flow pattern
2.2	4.29	1.95	5	1.71x10^5	Stratified
7.3	32.85	4.5	10	3.43 x10^5	Stratified
15.3	159.1	10.4	15	5.14 x10^5	Annular
25.6	689.7	24.6	20	6.86 x10^5	Churn

www.arpnjournals.com

CONCLUSIONS

This study aimed to provide some information about the droplet hydrodynamic and the flow behaviour in bend pipelines in order to find out the risk of hydrate blockage. The simulation results have been obtained using the VOF approach.

The effect of restart gas superficial velocity with fixed stagnant liquid level in the low section was investigated in 2D geometry. It is obvious that the liquid remaining in the low section of pipe decreases with an increase in gas superficial velocity and the amount of liquid depends on the fluid properties. Moreover, the flow pattern is also strongly dependent on the restart gas's superficial velocity as well as the amount of liquid in the low section.
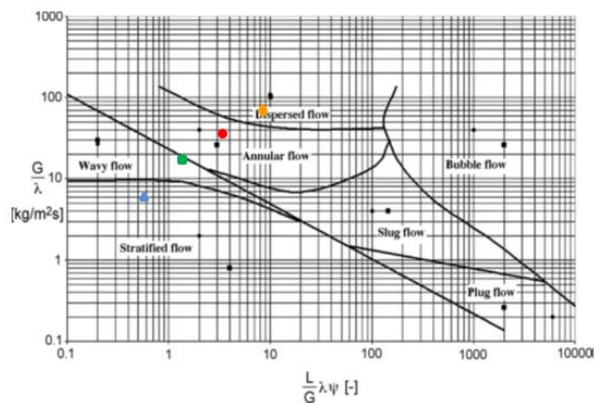
Figure-7. Comparison of flow pattern simulation with Baker flow map low patched liquid at different gas velocities, ▲ 5m/s, ■ 10m/s, ● 15m/s, and ♦ 20m/s.

A low gas superficial velocity with patched liquid of 0.2 m shows risk of hydrate formation due to the observed flow pattern, and is often a stratified flow. However, as the restart gas velocity is increased, regardless of initial liquid patching, hydrate blockage is less likely to be observed when the flow can be described as annular, churn or dispersed flow. Therefore, 2-D VOF model presented suitable result for the simulation of the flow pattern, which well compared with Baker flow map.

Further research will aim to examine the effect of fluid's properties, such as density and viscosity on the liquid displacement from the low section and the flow pattern. It is also necessary to conduct experimental work to determine the validity of the model more accurately, instead of using the flow map, which is generated for specific operating conditions and pipe sizes.

REFERENCES

[1] Baker D. 1954. Simultaneous Flow of Oil and Gas. Oil and Gas Journal. 53: 183-195.

[2] Barnea D., Shoham O., Taitel Y and Dukler A. E. 1980. Flow pattern transition for gas-liquid flow in horizontal and inclined pipes, International Journal of Multiphase Flow. 6: 217-225.

[3] Beggs H. and Brill J. P. 1973. A study of two-phase flow in inclined pipes, Journal of Petroleum Technology. 25: 607-617.

[4] Fitremann J. M. 1976. The stability of gas-flow over a stagnant liquid in a pipe and the onset of slugging. International Journal of Multiphase Flow. 3: 117-122.

[5] Grolman E., Commandeur N. C. J., BaatE. C. and Fortuin J. M. H. 1996. Wavy to slug flow transition in slightly inclined gas-liquid pipe flow, AIChE Journal. 42: 901.

[6] Kokal S. L. and Stanislav J. F. 1989. An experimental study of two phase flows in slightly inclined pipes: flow patterns, Chemical Engineering Science. 44(3): 665-679.

[7] Leporcher E., Kinnari K., Labes-carrier C., Maurel Ph. and Vandersippe W. 2002. Multiphase flow: Can we take advantage of hydrodynamic conditions to avoid hydrate plugging during deep-water restart operations? The SPE Annual Technical Conference and Exhibition, San Antonio, Taxes, 29 September-2 October.

[8] Volk M., Delle-Case E. and Estanga D. 2007. Risk-based restarts of untreated subsea oil and gas flowlines in the GoM. Technical Report, University of Tulsa.

[9] Woods B. D., HulburtE. T. and Hanratty T. J. 2000. Mechanism of slug formation in downwardly inclined pipes, International Journal of Multiphase Flow. 26: 977-298.

[10] Ranade V. 2002. Computational flow modelling for chemical reactor engineering. Academic press.

[11] Di Lorenzo M., Seo Y. and Soto G. S. 2011. The CSIRO'S hydrates flow loop as a tool to investigate hydrate behaviour in gas dominant flows. Proceedings of the 7th International Conference on Gas Hydrates (ICGH 2011), Edinburgh, Scotland, United Kingdom.

[12] Hart J., Hamersma P.J., Fortuin J.M.H. 1989. Correlations predicting frictional pressure drop and liquid holdup during horizontal gas-liquid pipe flow with a small liquid holdup. International Journal Multiphase Flow. 15(6): 947-96.

[13] Badie S., Hale C. P., Lawrence C. J. and Hewitt G. F. 2000. Pressure gradient and holdup in horizontal two-Phase gas-liquid flows with low liquid loading. International Journal of Multiphase Flow. 26: 1525-1543.